Nanosized Aluminum Altered Immune Function

Laura K. Braydich-Stolle,[†] Janice L. Speshock,[†] Alicia Castle,[†] Marcus Smith,[†,‡,§] Richard C. Murdock,[†] and Saber M. Hussain[†,*]

[†]Applied Biotechnology Branch, Human Effectiveness Directorate, Air Force Research Laboratory, Wright-Patterson AFB, Ohio, [‡]AFRL/RZPF, Wright-Patterson AFB, Ohio, and [§]Metals and Ceramics Division, University of Dayton Research Institute, Dayton, Ohio 45469

ABSTRACT On the basis of their uses in jet fuels and munitions, the most likely scenario for aluminum nanoparticle (NP) exposure is inhalation. NPs have been shown to be capable of penetrating deep into the alveolar regions of the lung, and therefore human alveolar macrophages (U937) with human type II pneumocytes (A549) were cultured together and exposed to NPs dispersed in an artificial lung surfactant to more accurately mimic the lung microenvironment. Two types of NPs were evaluated: aluminum (Al) and aluminum oxide (Al_2O_3). Following a 24-h incubation, cell viability was assessed using MTS, and mild toxicity was observed at higher doses with the U937 cells affected more than the A549. Since the U937 cells provided protection from NP toxicity, the cocultures were exposed to a benign concentration of NPs and infected with the respiratory pathogen community-associated methicillin-resistant *Staphylococcus aureus* (ca-MRSA) to determine any changes in cellular function. Phagocytosis assays demonstrated that the NPs impaired phagocytic function, and bacterial growth curves confirmed that this reduction in phagocytosis was not related to NP—bacteria interactions. Furthermore, NFκB PCR arrays and an IL-6 and TNF-α real time PCR demonstrated that both types of NPs altered immune response activation. This change was confirmed by ELISA assays that evaluated the secretion of IL-6, IL-8, IL-10, IL-1β, and TNF-α and illustrated that the NPs repressed secretion of these cytokines. Therefore, although the NPs were not toxic to the cells, they did impair the cell's natural ability to respond to a respiratory pathogen regardless of NP composition.

KEYWORDS: nanotoxicity · nanoparticle · aluminum · inflammatory response · immune response

Nanoenergetic aluminum has potential military, medical, and industrial applications,[1,5] yet very few studies have evaluated the risk associated with these materials. Currently, studies pertaining to the biological interactions of aluminum nanoparticles (Al NPs) are very limited. Previously, we demonstrated that Al_2O_3 NPs reduce cell viability in male germline stem cells in a concentration-dependent manner.[6] In another study we identified that the surface coating alters the toxicity in rat alveolar macrophages.[7] Currently, nanotoxicity studies performed using a wide range of nanomaterials in a variety of cellular models have demonstrated a dose-dependent effect, but one limitation from all of these studies is that realistic human exposure scenarios that describe what interactions occur following low levels of nanoparticle exposure have not been addressed. We cannot assume that just because the NPs are not killing a cell that the cell remains unaffected by their presence. Additionally, using unicellular *in vitro* models to represent complex tissues such as the lungs will not provide an exact depiction of how a multicellular tissue will respond, especially because many of the major organs within the body contain phagocytic cells to respond to localized damage (summarized in Table 1). However, *in vitro* cultures are useful for providing a preliminary foundation for studies to assess dosing ranges and probable mechanisms of toxicity and to allow the for the refinement of techniques before progressing to costly *in vivo* studies. Perhaps, a better *in vitro* scenario would be to produce cocultures of cells that include the immune cells that would be present to respond to the nanomaterials, providing an even more realistic *in vitro* scenario. The aim of this study was to examine the effects of Al NPs in an alveolar coculture model consisting of epithelial and immune cells, since ultrafine particles are found in pollution that can be easily inhaled and absorbed systemically and the majority of nanotoxicity studies have focused on lung exposure. Another objective of this study was to evaluate the changes

TABLE 1. Phagocytic Cells Located in Different Organ Systems

organ	phagocytic cell type
bone	osteoclast
brain	microglia
kidney	mesangial cells
liver	Kupffer cells
lung	macrophages
spleen	macrophages
skin	Langerhans cells

*Address correspondence to saber.hussain@wpafb.af.mil.

Received for review November 23, 2009 and accepted June 22, 2010.

Published online July 1, 2010. 10.1021/nn9016789

in cellular function following a nontoxic exposure to Al NPs. Since the coculture model employed epithelial and immune cells, immune function was evaluated by infecting the cocultures with a bacteria following NP exposure. The bacterial strain we chose to study was USA300 community-associated methicillin-resistant *Staphylococcus aureus* (ca-MRSA) because it can be a respiratory pathogen and military recruits[8] were identified by the Centers for Disease Control and Prevention (CDC) as an "at risk" group. Furthermore, the Al NPs were dispersed in artificial lung surfactant[9] to mimic the physiological fluid they would encounter in an *in vivo* scenario.

RESULTS AND DISCUSSION

Aluminum Nanoparticle Characterization. Since nanotoxicity is a relatively new field, a standard practice for testing of these materials has yet to be agreed upon. Early nanotoxicity studies did not report detailed characterization of the nanomaterials being evaluated, and therefore nanotoxicity studies have been subject to criticism. *In vitro* models have been judged for their lack of reproducibility, and a study by Sayes and colleagues has shown that in the case of lung exposure, *in vitro* models did not correlate well with *in vivo* models.[10] However, *in vivo* studies have also yielded conflicting toxicity data.[11−16] One study concluded that ultrafine TiO_2 particles (29 nm) increased inflammation and altered macrophage chemotactic responses in rat lungs, when compared to TiO_2 particles that were 250 nm.[13] However, another study showed that in rats, exposure to nanoscale TiO_2 rods/dots produced inflammatory responses that were not different from pulmonary effects of larger TiO_2 particles,[14] but rather toxicity was due to surface properties.[15,16] These studies used the same delivery method but varied drastically in the NP source, amount of NPs exposed, and the time of exposure, which could account for differences. Several studies have demonstrated that dispersion of nanomaterials in aqueous solutions altered the physiochemical properties of the nanomaterials, and this alteration was dependent on the different components of the solution and in turn varied the biological responses.[17] Thus, since these studies did not report nanomaterial characterization once they were in aqueous solution and given that the properties of nanomaterials can change when they go from a dry environment to an aqueous environment, this could account for the variability in the data. On this basis, questionable study designs and lack of characterization are the most likely sources of nonreproducible and potentially inaccurate results. Therefore, characterization is imperative in evaluating the biological interactions of nanomaterials, and researchers must identify these changes since they correlate to how a biological system is impacted. In Figure 1A and B the spherical morphology of the Al NPs was illustrated, and the TEM analysis measurements determined that the nanoparticles had relatively similar size distributions ranging from 32.7 ± 28.3 to 48.1 ± 21.0 nm (Table 2). After the NPs had been dispersed in water and then diluted in media, the Al_2O_3 demonstrated higher agglomeration in media without serum when compared to media with serum (859 ± 0.3 and 309 ± 0.4 nm, respectively). In addition, prior to cellular exposure, the NPs were dispersed in an artificial lung surfactant (ALS)[9] to determine the impact that the biological fluids would have on the nanomaterials and how this could relate to exposure. Once the NPs had been dispersed in the artificial lung surfactant, a similar trend was also observed with the Al_2O_3 NPs agglomerating to 878 ± 0.5 nm in exposure media and 486 ± 0.6 nm in growth media. The Al_2O_3 NPs dispersed in ALS and then placed in exposure and growth media aggregated to an average size of 859 ± 0.3 and 309 ± 0.4 nm, respectively (Table 2). In contrast, the Al NPs had an aggregate size of 698 ± 0.6 nm in exposure media, and in growth media the aggregate size increased to 839 ± 0.7 nm (Table 2). Moreover, one study from our laboratory has demonstrated that the chemical composition of the nanomaterials can change within the different solvents, and therefore it is important to determine the chemical composition following dispersion to identify the exact chemical nature of the nanoparticles that a biological system encounters. Following the dispersion in water and ALS, X-ray diffraction (XRD) patterns were compared to the XRD patterns obtained from the dry nanomaterials. These XRD patterns demonstrated that there was no change for both the Al and Al_2O_3 NPs, confirming that the NP chemical composition remained stable following dispersion and the cells were being exposed to Al and Al_2O_3 NPs (Figure 1C and D, respectively). However, it is important to note that Al is highly reactive, and therefore, the Al NPs were passivated with a 2−3 nm oxide layer by NovaCentrix to reduce the reactivity. Therefore, the surface chemistry of the NPs was similar, yet the core of the NP was different.

Currently, not all nanoparticles are created equal, and this concept has been reviewed by Hussain and colleagues.[18] Critical questions highlighted in this review were "For example, if two nano-sized silver powders are produced from two separate manufacturers employing two different techniques, can they still be considered identical? What characteristics are likely to vary from one manufacturer to the other? Could these differences lead to changes in biological interactions?" Additionally, another report comparing four different carbon black samples demonstrated that there were differences in toxicity results (using multiple end points for analysis) from four different carbon black samples obtained from three different manufacturers .[19] In light of these reports, characterization proves to be a major challenge in evaluating the biological effects of nanomaterials, and therefore it is essential to characterize each material prior to initiating biological studies.

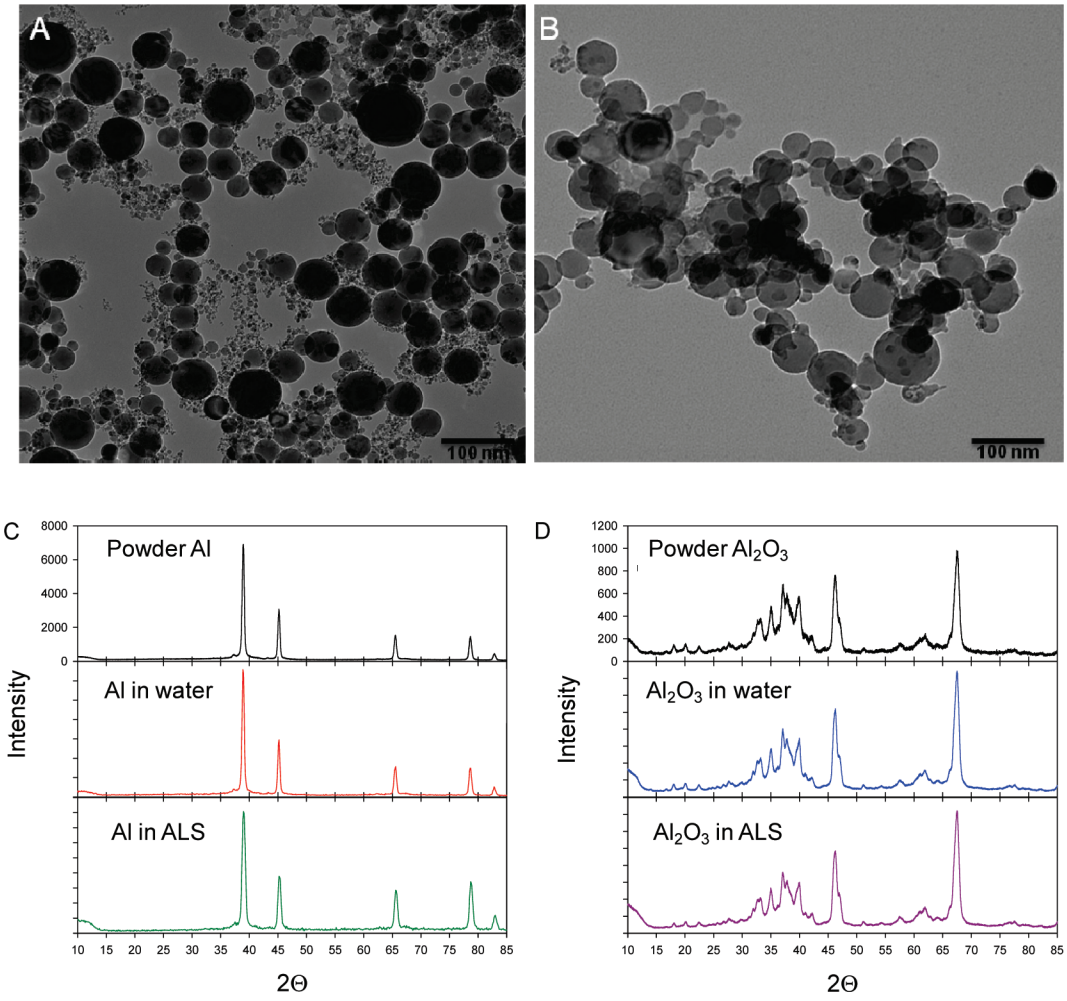

Figure 1. Characterization of aluminum nanoparticles. (A) TEM image of Al_2O_3 NP. (B) TEM image of Al NP. (C) NP primay size distributions and agglomerate sizes. The NPs aggregated in the water and lung surfactant. Furthermore, the Al_2O_3 NPs demonstrated decreased agglomeration when serum proteins are present in the media. (C, D) XRD analysis of Al and Al_2O_3 NPs in powdered form and dispersed in water or artificial lung surfactant. The XRD analysis demonstrated that both the Al (C) and the Al_2O_3 (D) remained stable in the different solutions and did not change chemical composition.

Establishment of Alveolar Cocultures and Cellular Viability. A previous study demonstrated that nanoparticles (NPs) are capable of penetrating the alveoli deep in the lung.[20] Therefore, this study developed an *in vitro* model to mimic the alveolar microenvironment. The alveoli are composed of three cell types: type I alveolar cells, type II alveolar cells, and alveolar macrophages. Type I cells are epithelial cells responsible for gas exchange, type II cells produce a lung surfactant to create surface tension and can also differentiate into type I cells to repair damaged type I cells, and the macrophages are the resident immune cells that are responsible for protecting the other cells. Since the NPs can penetrate the type I cells, the *in vitro* model we developed assessed the impact of the nanoparticles on the type II and macrophage cell types, especially since the macrophages respond to foreign material and the type II cells are essential for repairing any damage to the alveoli. The U937 cells are a monocyte cell line that can be stimulated to produce macrophages, and these cells secrete a variety of cytokines and chemokines constitutively or in response to stimuli, making them an ideal cell type for immune function studies. Furthermore, the A549 cells are type II alveolar cells and have been character-

TABLE 2. Nanoparticle Size Distribution of Aluminum Nanoparticles

		DLS Z-ave (d.nm) ± PdI					
		dispersion in water			dispersion in artificial lung surfactant		
sample	primary nanoparticle size TEM (nm)	media without serum	media with serum	ζ potential (mV)	media without serum	media with serum	ζ potentialqa (mV)
Al	48.08 ± 21.0	859 ± 0.3	309 ± 0.4	−15.2	878 ± 0.5	486 ± 0.6	
Al_2O_3	32.71 ± 28.3	698 ± 0.6	839 ± 0.7	38	805 ± 0.5	948 ± 0.6	

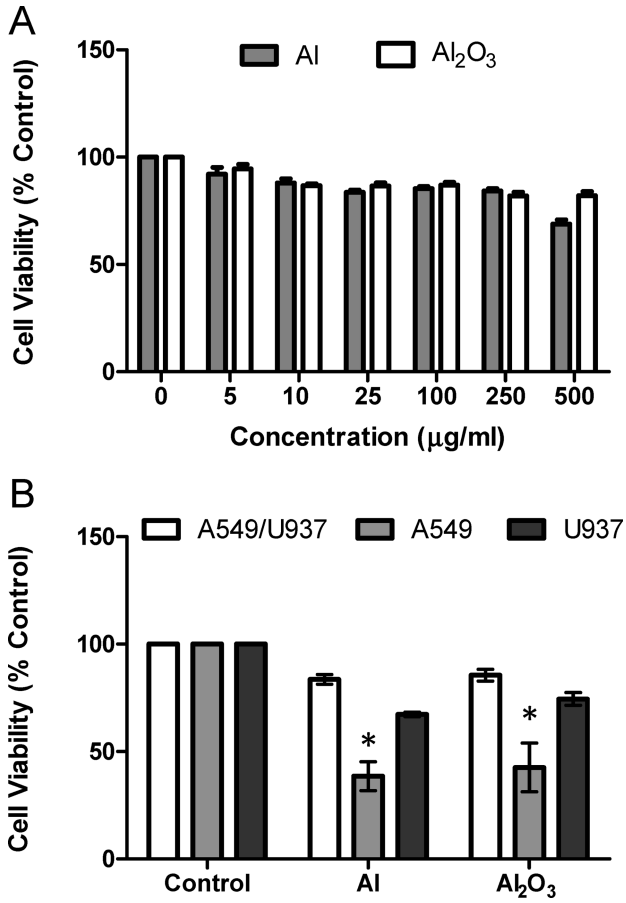

Figure 2. Cytotoxic effect of the aluminum nanoparticles in the alveolar coculture and single cell cultures. (A) Changes in cell viability in the alveolar coculture after 24 h of exposure to different concentrations of Al NPs. (B) Cell viability following a 24-h treatment with 25 μg/mL of Al NPs in the coculture as well as the single cultures. (Represents three independent trial; * denotes $p < 0.05$).

ized as a type II pulmonary model useful for drug studies,[21] making them an ideal candidate for nanoparticle studies. The A549 and the U937 cell lines were cultured in a ratio of 3 A549 cells to 1 U937 cell on the basis of the lung cellular ratios described by Wang *et al.*[22]

The human alveolar cocultures were exposed to NPs at concentrations ranging from 0−500 μg/mL, and then cell viability was assessed by evaluating mitochondrial function (Figure 2A). The NPs were relatively nontoxic in the cocultures with only minor changes in cell viability observed, mainly at the higher concentrations, which was likely a result of turbidity. In order to determine which cells were being affected in the cocultures, a live cell/dead cell assay was used, and this demonstrated that the macrophages were more susceptible to the NPs than the epithelial cells (data in Supporting Information), which was expected since the macrophages actively engulf foreign material in order to protect the epithelial cells. There have not been many reports on the exposure to aluminum nanoparticles; however, studies with 1.2-μm Al have shown that brief weekly exposures of individuals to Al dust resulted in scarring throughout the lungs.[23] Other studies have demonstrated that inhaled nanoparticles accumulated in the lungs and clearance was hindered during chronic exposure.[24] On the basis of these findings, we can anticipate that if the micrometer-sized particles caused lung problems, nanosized Al, which is more reactive and can penetrate deeper into the lungs, should produce an effect. The effect will become more pronounced over time as a result of clearance of the NP from the lungs being impeded. Currently, OSHA reports 15 mg/m^3 as a permissible exposure limit to aluminum within an 8-h time frame. This reported value is based on the assumption that not all of the aluminum will penetrate to the lungs and that it will also be cleared by the body and excreted in urine. Nanomaterials have been shown to penetrate deep into the lungs and to not clear the lungs, so chronic exposure can lead to accumulation. Using an equation to calculate the daily exposure based on this value, an average worker would be exposed to 3.9 μg/mL in 1 day (Supporting Information), and the 25 μg/mL represents approximately 1 week of exposure.

When the cell viability of the coculture was compared to the cell viability of the unicellular cultures, there was a significant difference in how both cell types responded to the nanoparticles. The A549 epithelial cells demonstrated significant cell death when the immune cells were not present, and the U937 also showed significant loss of viability (Figure 2B). When the cell viability of the coculture was compared to the cell viability of the unicellular cultures, no significant reductions in the cell viability of the epithelial cell was observed, whereas minor reduction in cell viability was observed for the macrophages, regardless of nanoparticle chemical composition. This data demonstrated that within the cocultures the immune cells were protecting the epithelial cells from NP toxicity, which would be expected *in vivo*, thus confirming that the *in vitro* coculture provided a better model than the individual cultures.

Cellular Function Assay. Additionally, because the main function of macrophages is to destroy foreign material, we assessed if the macrophages could still phagocytose the bacteria ca-MRSA after treatment with the NPs. Our data illustrated that the Al_2O_3 NPs did not impair phagocytosis, whereas the phagocytosis was impaired by the Al NPs (Figure 3A). A similar trend in phagocytic activity was previously observed where Al but not Al_2O_3 NPs reduced phagocytic function in rat alveolar macrophages.[7] Furthermore, neither Al NP altered the growth of the ca-MRSA cultures treated with the NPs (Figure 3B), suggesting that the change in the amount of bacteria phagocytosed was related to the macrophage function and not any NP−bacteria interactions. To conclude that the Al NPs were not affecting the bacteria directly and were indeed altering cell function, the Al NPs were topically added to bacterial growth agar to determine the minimum inhibitory concentration (MIC).

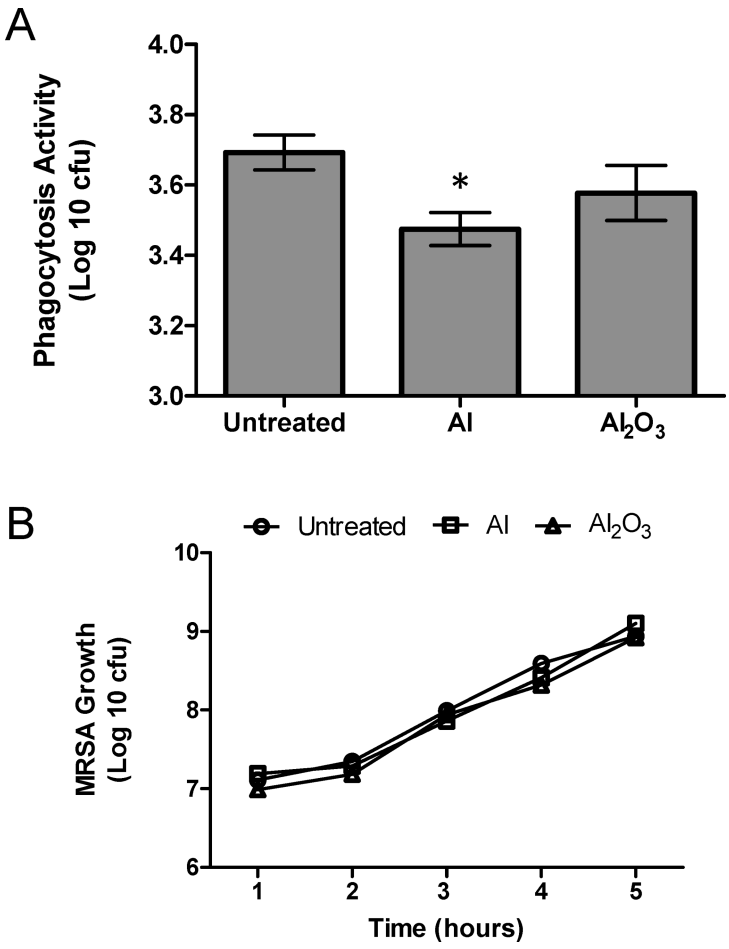

Figure 3. Impact of aluminum nanoparticles on ca-MRSA phagocytosis and growth. (A) Phagocytosis of ca-MRSA following a 24-h exposure to aluminum nanoparticles. (B) ca-MRSA growth in the presence of aluminum nanoparticles. (Represents four independent trials; * denotes $p < 0.05$).

There was no decline in bacterial numbers following overnight incubation when ca-MRSA was exposed to Al NP concentrations up to 1 mg/mL, indicating that the NPs are not bactericidal against this specific strain of bacteria (Supporting Information, Figure S1). Gentamicin (50 μg/mL) was used as a positive antibiotic control to confirm that the topical addition of the treatments was successful (Supporting Information, Figure S1). Since the bacteria were not being affected by the aluminum nanoparticles, a possible explanation for reduced phagocytosis is that the aluminum nanoparticles were chemically altering the cellular environment. Under normal conditions aluminum does not corrode, which is due to a thin protective oxide layer that forms on the surface of the metal. However, in an acidic environment aluminum oxide will react and form aluminum ions and water. Because the nanoparticles were taken up in the macrophages through phagocytosis, the end result of this phase is fusion with the lysosome. The localization within the lysosome was confirmed (Supporting Information Figure S2C), and because this organelle is acidic as a result of the presence of nitrous acid, it is likely that the NPs released Al ions. Furthermore, we suspect that due to the differences in the thickness of the oxide and the core metal within the nanoparticle the nitrous acid degraded the thin oxide coating on the Al NPs more quickly than on the Al_2O_3 NPs and uncovered the aluminum core, allowing more aluminum to be available to react within the macrophage. Additionally, if these aluminum ions in turn reacted with the nitrous acid in the lysosomes, one of the products for this reaction would be hydrogen ions. These hydrogen ions would alter the pH and ultimately disrupt the phagocytic process, which has been shown to be sensitive to fluctuations in pH.[25]

Evaluation of the Immune Response. Immunity is the body's natural defense against the invasion of foreign material. Major players in the body's innate immune response are localized phagocytic cells, which patrol the body seeking foreign materials and actively engulfing anything seen as nonself. During infection, the resident phagocytic and epithelial cells will secrete chemokines to recruit adaptive immune cells and cytokines to activate recruited cells for a more fastidious response to the foreign material. Because our phagocytosis data demonstrated that there was a change in macrophage function when a pathogen was present, further investigations into the normal immune responses were performed.

We chose to evaluate the impact that the Al NPs had on the NFκB pathway since this is a key regulator of immune function and regulates both innate and adaptive immunity. The ca-MRSA strain causes necrotizing pneumonia, necrotizing faciitis, and toxic shock syndrome in otherwise healthy individuals[26] through activation of the NFκB pathway. Activating the NFκB pathway also lyses macrophages and damages lung epithelium, causing an overwhelming release of pro-inflammatory cytokines, such as interlukein-6 (IL-6), interlukein-1β (IL-1β), and tumor necrosis factor α (TNF-α) (Figure 4A).[27,28] Therefore, the lung cocultures were treated with a low dose of NPs and then infected with the respiratory pathogen ca-MRSA to determine changes in gene expression for the NFκB pathway (Table 3) as well as targets of the NFκB pathway, inflammatory cytokine genes (Figure 5), and secretion of inflammatory cytokines (Figure 6).

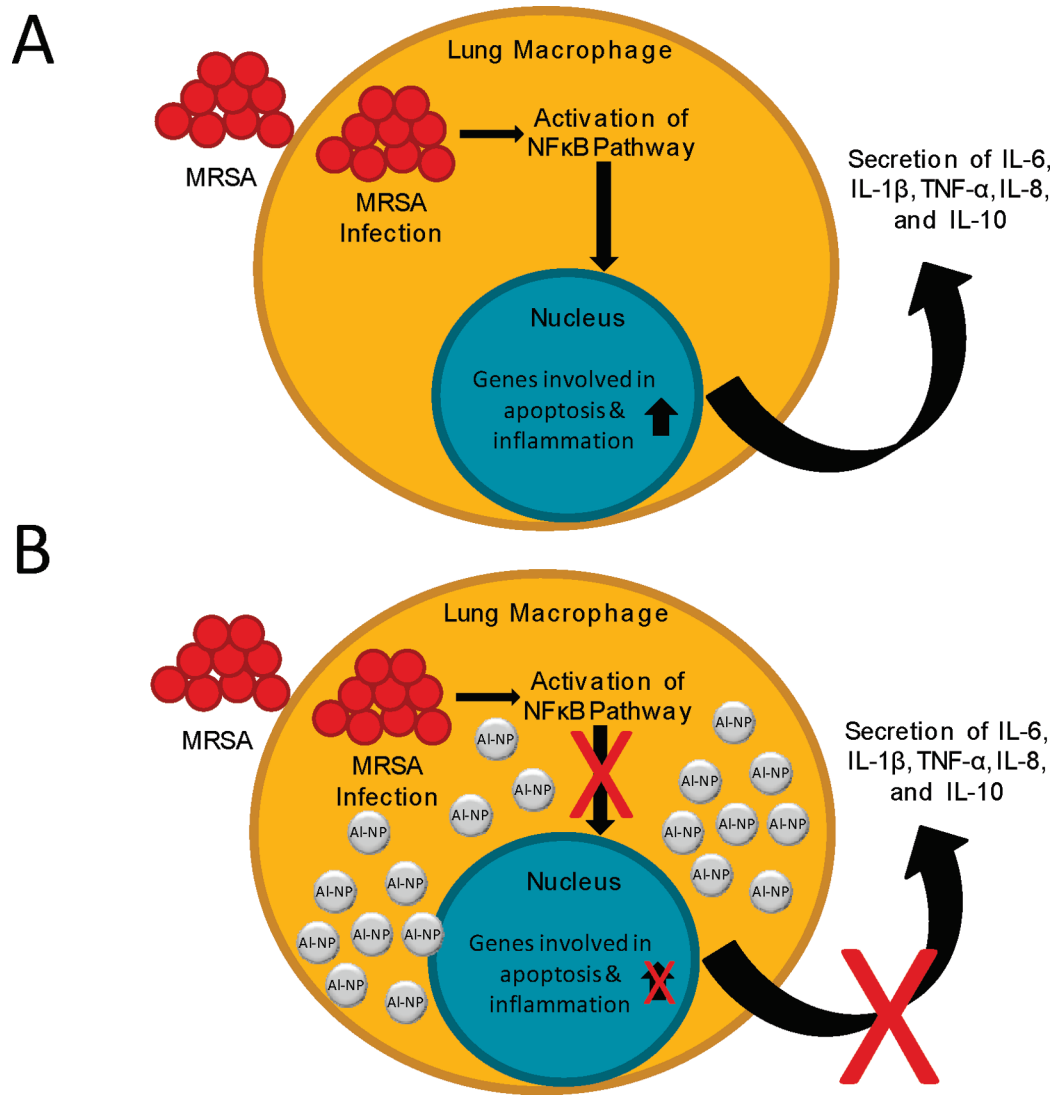

Figure 4. Macrophage response to ca-MRSA in the absence and presence of aluminum nanoparticles. (A) The typical response illicted by ca-MRSA infection in alveolar macrophages. (B)The observed response when aluminum nanoparticles were present during the ca-MRSA infection.

Changes in gene expression for the NFκB pathway are listed in Table 2 and show that there was minor induction of the NFκB pathway by the Al_2O_3 NPs alone but not the Al NPs. Furthermore, the ca-MRSA stimulated a strong activation of the NFκB pathway as anticipated; however, when the Al and Al_2O_3 NPs were present, the cells were unable to generate activation of the NFkB pathway in the presence of CA-MRSA. This data illustrated that the NPs alter or abolish the cells' ability to respond to a pathogen *via* the NFκB pathway. Inflammatory markers IL-6 and TNF-α, which are known to be activated by ca-MRSA, were evaluated after a 4-h and 6-h infection to determine if the suppression of the NFκB pathway altered gene expression of inflammatory cytokines (Figure 5). The data illustrated that after a 4-h infection with CA-MRSA IL-6 was up-regulated 8-fold and TNF-α 6.5-fold and the NPs alone did not generate an inflammatory response. Furthermore, when the NPs were present during the MRSA infection, the expression of IL-6 and TNF-α was abolished (Figure 5A). Additionally, gene expression was evalu-

TABLE 3. Activation and Regulation of NFκB Genes Following Exposure to Aluminum Nanoparticles and Stimulation with ca-MRSA[a])

	fold change (% control)				
gene symbol	MRSA	MRSA Al_2O_3	MRSA Al	Al_2O_3	Al
MALT1	1.83				
MAP3K1	−10.87				
MYD88	1.45				
RELB	7.08				
TMED4	1.82		3.00		
TNF	−4.56			13.01	
TNFAIP3	−2.08				
TNFRSF10B	1.91				

[a]Represents three independent trials, and gene changes from the PCR array with $p < 0.05$ are reported.

ated after 6 h, and the ca-MRSA alone treatments demonstrated a similar trend with IL-6 and TNF-α being up-regulated 5- and 2.5-fold, respectively. In contrast, IL-6 was down-regulated 2.8- and 2.08-fold by the Al_2O_3 and Al NPs, respectively. In the ca-MRSA−Al_2O_3 NPs IL-6 was down-regulated 2.4-fold, and in the ca-MRSA−Al NP 4-fold. In contrast, the TNF-α was down-regulated 1.5-fold for the Al_2O_3 NP treatment group and 2.15-fold for the Al NP treatment. When ca-MRSA was added to the cultures for 6 h, there was no significant expression of TNF-α (Figure 5B). The down-regulation of IL-6 in the treatment groups compared to the control group indicated that the expression of IL-6 was being repressed by the NPs. Furthermore, TNF-α was down-regulated in the NP alone treatments, and there was no significant expression in the ca-MRSA NP treatments, again suggesting repression of the immune system in the presence of Al NPs. This data indicated that the changes observed in the NFκB activation and regulation was carried through downstream to the inflammatory cytokine expression levels.

To further confirm the gene expression inflammatory response data and the loss of the immune response, ELISAs were performed on the common cytokines secreted by the macrophages. ca-MRSA typically activates the pro-inflammatory cytokines IL-6, IL-1β, and TNF-α, which are responsible for activating the endothelium for recruitment and differentiating and activating the recruited adaptive immune cells. The ca-MRSA initiated a 7.5-fold increase in the secretion of IL-6 in the lung cocultures when compared to control cells after a 6-h stimulation. ca-MRSA stimulated a 5-fold increase in the secretion of IL-1 β when compared to the control cells in the lung cocultures. The lung cocultures treated with ca-MRSA demonstrated a 22-fold increase in TNF-α secretion when compared to the control cultures. For all three pro-inflammatory cytokines, the increase in secretion that was observed after exposure to ca-MRSA was not seen when either of the Al NPs were present (Figure 6A−C) which should make the cells less able to fight infection. In addition, this trend was not observed following exposure to nanosized gold or aluminum nitride (AlN), indicating that it was a unique effect observed for the Al NPs (Supporting InformationFigure 3A−C). However in the case of ca-MRSA that produces the superantigen staphylococcal entertoxin B (SEB), which causes an uncontrolled release of pro-inflammatory cytokines to increase pathogenesis, the NP inhibitory effects could be beneficial. A similar trend was observed with the chemokine IL-8, which is responsible for recruiting polymorphonuclear leukocytes (PMN) to the site of infection to aid in killing pathogens. When ca-MRSA was present, secretion of IL-8 was up-regulated 12-fold. However, when the NPs were present IL-8 was not up-regulated, potentially leaving the cells more

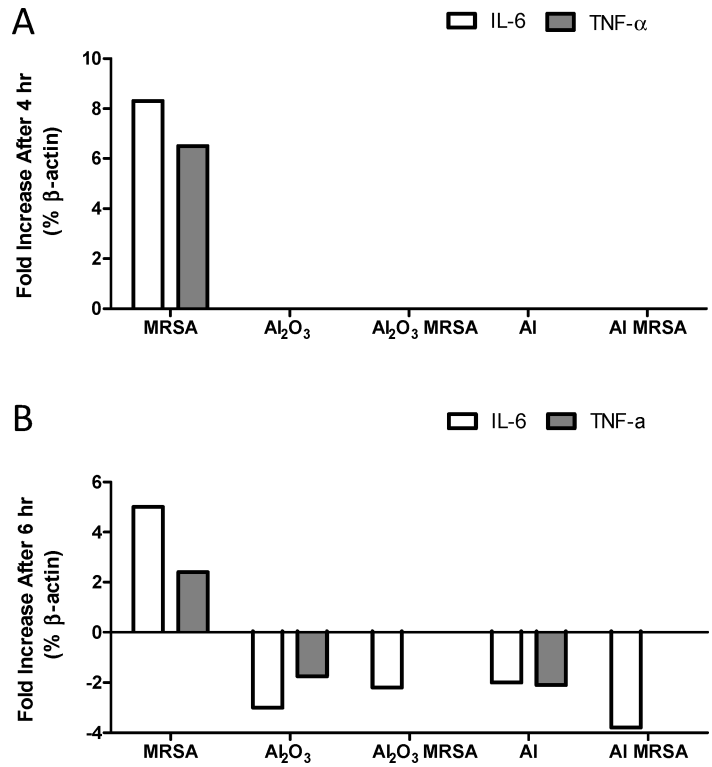

Figure 5. Evaluation of IL-6 and TNF-α gene expression following nanoparticle treatment and MRSA infection. (A) Expression of IL-6 and TNF-α following a 4-h infection with ca-MRSA. (B) Expression of IL-6 and TNF-α following a 6-h infection with ca-MRSA. (Represents three independent trials, and gene changes with $p < 0.05$ are reported).

vulnerable to the pathogen (Figure 6D). A similar trend was observed following treatment with the nanosized Au and AlN indicating that this response was not unique to the Al NPs (Supporting InformationFigure 3D). In addition, the NPs were shown to increase the down-regulation of IL-10 in the presence of ca-MRSA (Figure 6E). This anti-inflammatory cytokine is responsible for inhibiting the synthesis of pro-inflammatory cytokines and blocks NFκB activation, which initiates apoptosis, and ca-MRSA is known to cause necrosis. After stimulation with ca-MRSA, IL-10 was down-regulated 1.5-fold, and this decrease was even greater in the presence of the NPs with a 7-fold decrease by Al_2O_3 NP and a 20-fold decrease by the Al NP. However, for the Au NP and AlN treatments there was no change in IL-10 expression (Supporting InformationFigure 3E). In general, the NPs generated a significant alteration of the immune response by inhibiting activation of the NFκB pathway, which in turn impacted the expression targets of this pathway, such as inflammatory cytokines (Figure 4B). The key point to note here is that the inhibition of cytokine secretion related to the suppression of the NFκB pathway, and since this pathway was down-regulated in the presence of the Al NPs, all mechanisms of immune activation are altered, repressing any alternative activation of

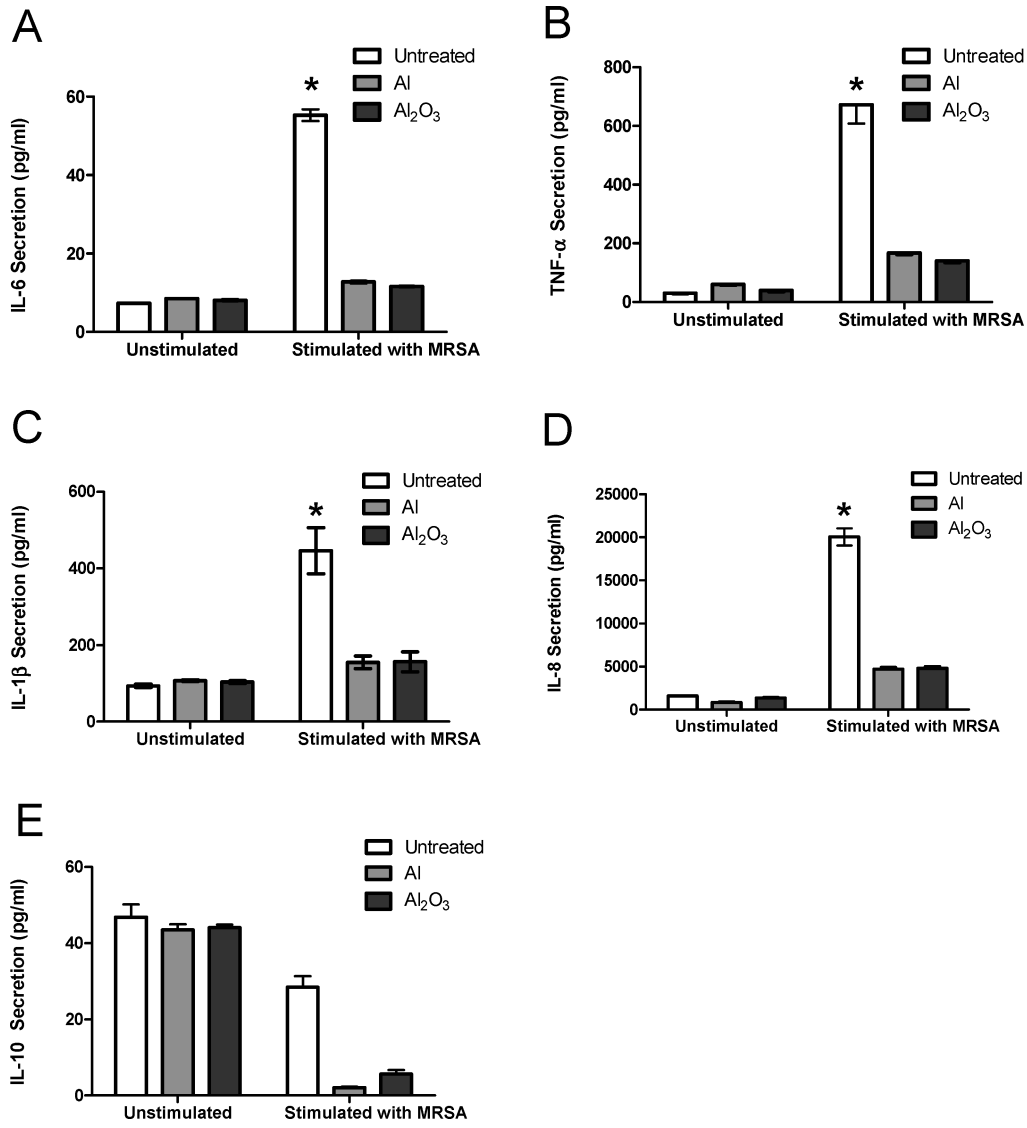

Figure 6. Secretion of inflammatory cytokines following exposure to aluminum nanoparticles and stimulation with ca-MRSA. (A−C) Secretion of pro-inflammatory cytokines: (A) IL-6 secretion, (B) IL-1β secretion, (C) TNF-α secretion. (D) Secretion of the chemokine IL-8. (E) Secretion of the anti-inflammatory cytokine IL-10. (Represents six independent trials.)

macrophages. In addition, since GM-CSF (granulocyte macrophage colony stimulating factor) is regulated by NFκB and is the major chemokine for macrophages and neutrophils, it is likely that recruitment of additional immune cells to the exposure site will be altered as well. Currently, the fate of Al NPs could follow two potential routes for toxicity: they could remain in the lungs or cross the gas exchange barriers and be incorporated into the bloodstream. In light of the fact that studies have demonstrated that clearance of NPs from the lungs was impeded, the most likely scenario would be that the Al would persist in the lungs and continue to be engulfed by macrophages.

CONCLUSIONS

In vitro models need to be validated as an accurate model for tissue representation prior to their use as a predictor of toxicity. This study demonstrated that the alveolar coculture provided a more comprehensive *in vitro* model in which to study the effects of NP exposure, since there was significant variation in the cellular response observed between the unicellular cultures and the coculture. Furthermore, a recent publication demonstrated the advantages of using 3D cultures over 2D cultures, yet the researchers only assessed one cell type.[29] In the future the best *in vitro* model system would be to merge the cocultures with the immune cells into a 3D culture matrix to yield a much more comprehensive model for studying the effects of nanomaterials before moving on to costly *in vivo* studies. Using the alveolar coculture model, we were able to demonstrate that the NPs did not impact cell viability in regard to the human alveolar cocultures or the CA-MRSA bacteria alone. However, just because the cells remained viable did not mean that they were unaltered by the presence of the NPs. When a respi-

ratory pathogen was introduced into these cocultures there was a difference in how these cells responded when the NPs were present. There was a reduction in the phagocytic ability of the immune cells, and changes in the immune response were observed when the NPs were present. Therefore, despite the low toxicity, the presence of the NPs changed the cells' natural ability to respond to a pathogen.

MATERIALS AND METHODS

Nanoparticles. The Al and Al_2O_3 NPs were received from NovaCentrix (formerly Nanotechnoloiges Inc.). The NPs were received in powdered form, weighed out, and dispersed in an artificial lung surfactant[9] to prepare 10 mg/mL working stock solutions. The NPs solutions to be used for dosing were made at the time of dosing to avoid any changes in the NPs. It is important to note that Al is highly reactive, and therefore the Al NPs were passivated with a 2−3 nm oxide layer by NovaCentrix to reduce the reactivity. Therefore, the surface chemistry of the NPs was similar, yet the core of the NP was different.

Nanoparticle Characterization. The average NP size was determined using TEM analysis for the powders and dynamic light scattering (DLS) for the aqueous solutions (both water and ALS) using previously described methods.[18] Furthermore, the chemical composition of the NPs was evaluated in the dry powdered form and after incubation in the water and artificial lung surfactant to determine if there were any changes from the exposure to the fluids. For the water and artificial lung surfactant study the NPs were dispersed in the appropriate solvent, bath sonicated, ultracentrifuged at 160 000 × *g*, and washed. Following the washes the NPs were dried. Powder diffraction (XRD) was then performed on the samples to yield the crystal pattern for the NPs. By comparing the dried fluid samples to the original powder, changes in chemical composition could be observed.

Human Lung Cocultures. In this study, the A549 cell line and the U937 cell line were chosen as an *in vitro* model for inhalation. To mimic the alveoli microenvironment, the A549 epithelial cells were cocultured with the U937 cells in a 3:1 (A549:U937)[22] ratio, and the NPs were dispersed in an artificial lung surfactant[9] prior to exposure. Both the A549 and the U937 cell lines were purchased from ATCC (CCL-185 and CRL-1593.2, respectively) and grown in RPMI-1640 media supplemented with 1% Pen-Strep and 10% heat-inactivated FBS. Prior to preparing the cocultures the U937 cells were stimulated with 100 ng/mL of phorbol-12-myristate-13-acetate (PMA) for 48 h to induce differentiation into macrophages. The A549 cells and the stimulated U937 cells were plated in the same tissue culture plates at a ratio of 3:1 (epithelial cells to macrophages). Twenty-four hours after plating the cocultures were dosed with the NPs for 24 h. For the PCR and ELISA studies, the cocultures were then infected with the CA-MRSA bacteria for 1−6 h following the NP treatment.

Bacteria Stocks. A USA300 strain of community-associated methicillin-resistant *Staphylococcus aureus* (ca-MRSA) was obtained as a primary isolate from Dr. Marcus Zervos at William Beaumont Hospital (Royal Oak, MI). An isolated colony was grown to mid-logarithmic phase in Todd Hewitt broth (Beckton, Dickinson and Company) supplemented with 0.2% yeast extract (Beckton, Dickinson and Company) (THYB) determined *via* optical density measurements using the Genesys 20 spectrophotometer (ThermoScientific) at a wavelength of 600 nm. The culture was diluted to 10^4 colony forming units per milliliter (cfu/mL) in sterile PBS supplemented with magnesium and calcium (Hyclone). The bacteria were added to the coculture cell model at a multiplicity of infection (MOI) of approximately 0.015 or to the macrophages alone at an MOI of 0.01. This dose was efficiently phagocytosed by the macrophages but was nontoxic within a five hour period.

Bacterial Growth Curve. The ca-MRSA was streaked onto trypticase soy agar supplemented with 5% sheep blood (Beckton, Dickinson and Company) upon receipt. A single colony was used to inoculate 10 mL of THYB. This culture was incubated overnight at 37 °C. Al or Al_2O_3 NPs were added to 10 mL of fresh THYB at 25 μg/mL, and the mixture was bath sonicated to distribute the NPs. Then, 200 μL of overnight culture was added to the NP-exposed THYB or plain THYB and was allowed to grow at 37 °C. The culture was grown over time with 100-μL aliquots being removed, diluted, and plated in triplicate every hour on THYB that was supplemented with 1.4% Bacto Agar (Beckton, Dickinson and Company) (THYA) and incubated overnight at 37 °C. The bacterial colonies were enumerated by physical counts. The data are represented as the average of four trials ± the standard deviation.

Phagocytosis Assays. U937 cells were stimulated with PMA at 100 ng/mL and were seeded at 1×10^6 cells per well into 12-well tissue culture-treated plates. Following a 48-h incubation, the media containing PMA was removed from the cells, and following two washes with PBS, the cells were exposed to 25 μg/mL of 2 different Al NP formulations (Al and Al_2O_3) or to media (RPMI without serum) alone. Twenty-four hours post NP exposure, the cells were washed 2 times with PBS and were infected with ca-MRSA as described above. The cells were briefly centrifuged (500 × *g*, 1 min) to ensure efficient contact of the bacteria to the cells. The cells were incubated with the bacteria for 1.5 h at 37 °C with 5% CO_2, which was determined to be the amount of time required for maximal uptake (data not shown). Following the incubation, the cells were washed 2 times with PBS to remove unbound bacteria and were treated with 50 μg/mL of gentamicin (Invitrogen, Carlsbad, CA), which selectively kills the extracellular bacteria. After a 10 min exposure to gentamicin, the cells were lysed with sterile water, and the internalized bacteria were plated onto THYA and were grown overnight at 37 °C with 5% CO_2. The bacteria were enumerated manually with $n = 6$ per treatment. The data are represented as the average of four trials ± the standard deviation.

Cell Viability. The cocultures, the A549 cells, and the U937 cells were treated with varying concentrations (0−500 μg/mL) of aluminum nanoparticles for 24 h, and then cell viability was assessed using the MTS assay from Promega. The data are represented as the average of three trials ± the standard deviation.

PCR Arrays. The cocultures were treated with aluminum nanoparticles at a concentration of 25 μg/mL for 24 h and then infected with ca-MRSA at an MOI of 0.02 for 1 h. Following the infection with ca-MRSA, RNA was isolated from the samples using the RNA isolation kit from Qiagen. The RNA was then processed for PCR array analysis using the kits from SABiosciences (formerly SuperArray), and the human NFκB array was run according to the manufacturer's protocols. The data from the arrays were analyzed using SABiosciences analysis software. The data are represented as the average of three independent experiments ± the standard deviation, and gene changes were only reported if $p < 0.05$.

ELISAs. The cocultures were treated with aluminum nanoparticles at a concentration of 25 μg/mL for 24 h and then infected with ca-MRSA at an MOI of 0.02 for 1 h. Following the infection with ca-MRSA, the media was removed from the cocultures, and the presence of IL-6, IL-8/NAP-1, IL-10, IL-1β, and TNF-α were all analyzed using the human ELISA kits from BIOSOURCE according to the manufacturer's protocols. The data are represented as the average of six individual trials run in triplicate ± the standard deviation.

Acknowledgment. This work was supported through an NST Nanoenergetic Effort through the Air Force Research Laboratories in collaboration with C. Bunker. L.K.B.-S. is funded through the Henry Jackson Foundation, J.L.S. through a postdoctoral fellowship from the Defense Threat Reduction Agency-National Research Council, A.C. by the Consortium of Research Fellows Program, and M.S. through a Dayton Area Graduate Studies Institute fellowship.

Supporting Information Available: Explanation for the dosing concentrations, determination of the minimal inhibitory concentration for the ca-MRSA bacteria, nanoparticle localization studies, and gold nanoparticle and aluminum ion inflammatory response studies. This material is available free of charge *via* the Internet at http://pubs.acs.org.

REFERENCES AND NOTES

1. Hunley. J. D. American Institute of Aeronautics and Astronautics, Presented as an Invited Paper at the 35th AIAA, ASME, SAE, ASEE Joint Propulsion Conference and Exhibit, 1999.
2. Miziolek, A. Nanoenergetics: An Emerging Technology Area of National Importance. *AMPTIAC Q.* **2002**, *6*, 4348.
3. Tyner, K. M.; Schiffman, S. R.; Giannelis, E. P. Nanobiohybrids as Delivery Vehicles for Camptothecin. *J. Controlled Release* **2004**, *95*, 501–514.
4. Monteiro-Riveiere, N. A.; Oldenbury, S. J.; Inaman, A. O. Interactions of Aluminum Nanoparticles with Human Epidermal Keratinocytes. *J Appl. Toxicol.* **2010**, *30*, 276–285.
5. Department of Defense Director, Defense Research and Engineering. Defense Nanotechnology Research and Development. 2005, 4 January 2006; http://www.nano.gov/html/res/DefenseNano2005.pdf.
6. Braydich-Stolle, L. K.; Hussain, S. M.; Schlager, J. J.; Hofmann, M. C. In Vitro Cytotoxicity of Nanoparticles in Mammalian Germline Stem Cells. *Toxicol. Sci.* **2005**, *88*, 412–419.
7. Wagner, A. J.; Bleckmann, C. A.; Murdock, R. C.; Schrand, A. M.; Schlager, J. J.; Hussain, S. M. Cellular Interaction of Different Forms of Aluminum Nanoparticles in Rat Alveolar Macrophages. *J. Phys. Chem. B* **2007**, *111*, 7353–7359.
8. Zinderman, C. E.; Conner, B.; Malakooti, M. A.; LaMar, J. E.; Armstrong, A.; Bohnker, B. K. Community-Acquired Methicillin-Resistant Staphylococcus aureus Among Military Recruits. *Emerging Infect. Dis.* **2004**, *10*, 941–944.
9. Ansoborlo, E.; Heng-Napoli, M. H.; Chazel, V.; Gibert, R.; Guilmette, R. A. Review and Critical Analysis of Available in Vitro Dissolution Tests. *Health Phys.* **1999**, *77*, 638–645.
10. Sayes, C. M.; Reed, K. L.; Warheit, D. B. Assessing Toxicity of Fine and Nanoparticles: Comparing in Vitro Measurements to in Vivo Pulmonary Toxicity Profiles. *Toxicol. Sci.* **2007**, *97*, 163–180.
11. Lam, C. W.; James, J. T.; McCluskey, R.; Hunter, R. L. Pulmonary Toxicity of Single Walled Carbon Nanotubes in Mice 7 and 90 Days after Intratracheal Instillation. *Toxicol. Sci.* **2004**, *77*, 126–134.
12. Warheit, D. B.; Laurence, B. R.; Reed, K. L.; Roach, D. H.; Reynolds, G. A.; Webb, T. R. Comparative Pulmonary Toxicity Assessment of Single Walled Carbon Nanotubes in Rats. *Toxicol. Sci.* **2004**, *77*, 117–125.
13. Renwick, L. C.; Brown, D.; Clouter, A.; Donaldson, K. Increased Inflammation and Altered Macrophage Chemotactic Responses Caused by Two Ultrafine Particle Types. *Occup. Environ. Med.* **2004**, *61*, 442–447.
14. Warheit, D. B.; Webb, T. R.; Sayes, C. M.; Colvin, V. L.; Reed, K. L. Pulmonary Instillation Studies with TiO_2 Rods and Dots in Rats: Toxicity Is Not Dependent upon Particle Size and Surface Area. *Toxicol. Sci.* **2006**, *91*, 227–236.
15. Warheit, D. B.; Webb, T. R.; Reed, K. L.; Frerichs, S.; Sayes, C. M. Pulmonary Toxicity Study in Rats with Three Forms of Ultrafine-TiO_2 Particles: Differential Responses Related to Surface Properties. *Toxicology* **2007**, *230*, 90–104.
16. Warheit, D. B.; Webb, T. R.; Colvin, V. L.; Reed, K. L.; Sayes, C. M. Pulmonary Bioassay Studies with Nanoscale and Fine-Quartz Particles in Rats: Toxicity Is Not Dependent Upon Particle Size but on Surface Characteristics. *Toxicol. Sci.* **2007**, *95*, 270–280.
17. Murdock, R. C.; Braydich-Stolle, L. K.; Schrand, A. M.; Schlager, J. J.; Hussain, S. M. Characterization of Nanomaterial Dispersion in Solution Prior to In Vitro Exposure Using Dynamic Light Scattering Technique. *Toxicol. Sci.* **2007**, *101*, 239–253.
18. Hussain, S.; Braydich-Stolle, L. K.; Schrand, A. M.; Murdock, R. C.; Yu, K. O.; Mattie, D. M.; Schlager, J. J.; Terrones, M. Toxicity Evaluation for Safe Use of Nanomaterials: Recent Achievements and Technical Challenges. *Adv. Mater.* **2009**, *21*, 1549–1559.
19. Monterio-Riveria, N. A.; Inman, A. O. Challenges for Assessing Carbon Nanomaterials Toxicity to the Skin. *Carbon* **2006**, *44*, 1070–1078.
20. Oberdorster, G.; Oberdorster, E.; Oberdorster, J. Nanotoxicology: An Emerging Discipline Evolving from Studies of Ultra-fine Particles. *Environ. Health Perspect.* **2005**, *113*, 823–839.
21. Foster, K. A.; Oster, C. G.; Mayer, M. M.; Avery, M. L.; Audus, K. L. Characterization of the A549 Cell Line as a Type II Pulmonary Epithelial Cell Model for Drug Metabolism. *Experimental Cell Research* **1998**, *243* (2), 359–366.
22. Wang, S.; Young, R. S.; Sun, N. N.; Witten, M. L. Toxicology: In Vitro Cytokine Release From Type II Pneumocytes and Alveolar Macrophages Following Exposure to JP-8 Jet Fuel in Co-Culture. *Toxicology* **2002**, *173*, 211–219.
23. Hathaway, G. J.; Proctor, N. H.; Hughes, and J. P.; Fischman, M. L. *Proctor and Hughes' Chemical Hazards of the Workplace*; VanNostrand Reinhold: New York, 1991.
24. Moller, W.; Felten, K.; Sommerer, K.; Scheuch, G.; Meyer, G.; Meyer, P.; Haussinger, K.; Kreyling, W. G. Deposition, Retention, and Translocation of Ultrafine Particles from the Central Airways and Lung Periphery. *Am J. Respir. Crit. Care Med.* **2008**, *177*, 426–432.
25. Gargan, R. A.; Hamilton-Miller, J. M.; Brumfitt, W. pH dependent effects on *in vitro* phagocytosis in neutrophils. *Infect. Immun.* **1993**, *61*, 8–12.
26. Gillet, Y.; Issartel, B.; Vanhems, P.; Fournet, J.-C.; Lina, G.; Bes, M.; Vandenesch, F.; Piémont, Y.; Brousse, N.; Floret, D.; Etienne, J. Association Between Staphylococcus aureus Strains Carrying Gene for Panton-Valentine Leukocidin and Highly Lethal Necrotizing Pneumonia in Young Immunocompetent Patients. *Lancet* **2002**, *359*, 753–759.
27. Renwick, L.; Hardie, A.; Girvan, E. K.; Smith, M.; Leadbetter, G.; Claas, E.; Morrison, D.; Gibb, A. P.; Dave, J.; Templeton, K. E. Detection of Methicillin-Resistant Staphylococcus aureus and Panton-Valentine Leukocidin Directly from Clinical Samples and the Development of a Multiplex Assay Using Real-Time Polymerase Chain Reaction. *Eur. J. Clin. Microbiol. Infect. Dis.* **2008**, *27*, 791–796.
28. Kahl, B. C.; Peters, G. Mayhem in the Lung. *Science* **2008**, *315*, 1082–1083.
29. Lee, J.; Lilly, G. D.; Doty, R. C.; Podsiadlo, P.; Kotov, N. A. *In Vitro* Toxicity Testing of Nanoparticles in 3D Cell Culture. *Small* **2009**, *5*, 1213–1221.